Antiferromagnetism Induced by Bond Su-Schrieffer-Heeger Electron-Phonon Coupling: A Quantum Monte Carlo Study

Xun Cai,[1] Zi-Xiang Li,[2,3,4] and Hong Yao[1,5,*]

[1]*Institute for Advanced Study, Tsinghua University, Beijing 100084, China*
[2]*Beijing National Laboratory for Condensed Matter Physics & Institute of Physics, Chinese Academy of Sciences, Beijing 100190, China*
[3]*Department of Physics, University of California, Berkeley, California 94720, USA*
[4]*Materials Sciences Division, Lawrence Berkeley National Laboratory, Berkeley, California 94720, USA*
[5]*State Key Laboratory of Low Dimensional Quantum Physics, Tsinghua University, Beijing 100084, China*

(Received 18 February 2021; revised 22 May 2021; accepted 28 October 2021; published 10 December 2021)

Antiferromagnetism (AFM) such as Néel ordering is often closely related to Coulomb interactions such as Hubbard repulsion in two-dimensional (2D) systems. Whether Néel AFM ordering in two dimensions can be dominantly induced by electron-phonon couplings (EPC) has not been completely understood. Here, by employing numerically exact sign-problem-free quantum Monte Carlo (QMC) simulations, we show that bond Su-Schrieffer-Heeger (SSH) phonons with frequency ω and EPC constant λ can induce AFM ordering for a wide range of phonon frequency $\omega > \omega_c$. For $\omega < \omega_c$, a valence-bond-solid (VBS) order appears and there is a direct quantum phase transition between VBS and AFM phases at ω_c. The phonon mechanism of the AFM ordering is related to the fact that SSH phonons directly couple to electron hopping whose second-order process can induce an effective AFM spin exchange. Our results shall shed new light on understanding AFM ordering in correlated quantum materials.

DOI: 10.1103/PhysRevLett.127.247203

Introduction.—Electron-phonon coupling (EPC) exists ubiquitously in quantum materials. Moreover, it plays a crucial role in driving various exotic quantum phenomena, including charge-density wave (CDW) order [1,2], Su-Schrieffer-Heeger topological state [3,4], and, most notably, BCS superconductivity (SC) [5,6]. Since EPC normally induces an effective attraction between electrons, it has been well understood theoretically that EPC induces charge-density-wave, bond-density-wave, or conventional superconductivity in quantum systems, which was further illustrated in recent works [7–17]. Nonetheless, the role of EPC in driving antiferromagnetism (AFM) and unconventional SC in strongly correlated systems has been under debate since it is widely believed that repulsive Coulomb interactions between electrons are essential in developing AFM and unconventional SC (including high-temperature SC) [18–23].

In the past many years, increasing experimental and theoretical studies suggest that EPC can be an essential ingredient in understanding high-temperature SC, including cuprates [24–41] and iron-based superconductors [42–53], and in driving exotic orders such as pair-density wave [54], raising renewed interests in studying the role of EPC in correlated quantum systems. Since unconventional SC is often closely related to antiferromagnetism [18–23], it is natural to ask whether EPC can play any essential role in driving AFM ordering. Although various previous works have studied the competition between AFM order dominantly induced by the Hubbard interactions and other types of orders such as CDW induced by EPC [55–70], whether AFM ordering can be induced dominantly by EPC remains elusive.

In this Letter, we fill in the gap by showing that an AFM insulator can be dominantly induced by phonons. Specifically, we systematically study the square lattice

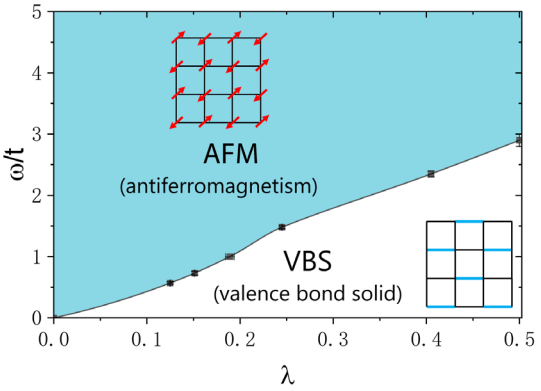

FIG. 1. The quantum phase diagram of the square lattice bond SSH model at half filling as a function of dimensionless electron-phonon-coupling (EPC) constant λ and phonon frequency ω. The insets depict AFM and VBS orders. The results are obtained by large-scale sign-problem-free zero-temperature QMC simulations. Note that the state with AFM ordering is degenerate with the state with pseudospin AFM ordering due to the O(4) symmetry of the model at half filling.

Su-Schrieffer-Heeger (SSH) optical phonon model at half filling by performing large-scale quantum Monte Carlo (QMC) simulations [71,72]. The simulations of the model can be rendered sign-problem-free so that we can access large system sizes to reach reliable results [73–79] (for a recent review of sign-free QMC, see Ref. [80]). Although acoustic and optical SSH phonon models have been studied by various theoretical and numerical approaches [81–95], it has not been shown that AFM ordering can be dominantly triggered by SSH phonons. By performing the first state-of-the-art zero-temperature QMC simulation on the 2D SSH model of optical phonons with frequency ω, we are able to obtain its reliable ground-state phase diagram as a function of ω and EPC constant λ, revealing that the AFM ordering emerges in a large portion of the phase diagram, as shown in Fig. 1. To the best of our knowledge, it is the first time that an AFM insulator is shown, in a numerically exact way, to be dominantly driven by EPC rather than by electron Coulomb repulsions. We would like to emphasize that the phonon mechanism of AFM ordering is intimately related to the fact that SSH phonons couple to electron hopping whose second-order process can induce an effective AFM spin exchange and drive an AFM ordering, as we explain.

Model.—We consider the bond SSH model [62] on the square lattice with the following Hamiltonian:

$$H = -t\sum_{\langle ij\rangle}(c_{i\sigma}^{\dagger}c_{j\sigma} + \text{H.c.}) + \sum_{\langle ij\rangle}\frac{\hat{P}_{ij}^2}{2M} + \frac{K}{2}\hat{X}_{ij}^2 + g\sum_{\langle ij\rangle}\hat{X}_{ij}(c_{i\sigma}^{\dagger}c_{j\sigma} + \text{H.c.}), \quad (1)$$

where $\langle ij\rangle$ refers to the bond between nearest-neighbor (NN) sites i and j, $c_{i\sigma}^{\dagger}$ creates an electron on site i with spin polarization $\sigma = \uparrow/\downarrow$, $\hat{X}_{ij}$ and $\hat{P}_{ij}$ are the displacement and momentum operators of the optical SSH phonons on the NN bond $\langle ij\rangle$. The chemical potential μ is implicit in the Hamiltonian and hereafter we shall focus on the case of half-filling by setting $\mu = 0$. Here t is the electron hopping amplitude and SSH phonon frequency is $\omega = \sqrt{K/M}$. The displacement field of SSH phonons is linearly coupled to the electron's NN hopping rather than to electron density. The strength of EPC can be characterized by the dimensionless EPC constant $\lambda \equiv [(g^2/K)/W]$, where $W = 8t$ is the characteristic band width of the square lattice. Hereafter, we set $t = 1$ as energy unit and set $K = 1$ by appropriately redefining $\hat{X}_{ij}$. Note that the bond SSH model is a member of the family of the Peierls models of electron-phonon coupling and it differs from nonbond SSH models [3,4,96]. Since acoustic SSH phonons can give rise to similar physics, we consider only optical SSH phonons here for simplicity.

It is worth noting that the bond SSH phonon model at half filling described by Eq. (1) respects the $\mathrm{SO}(3) \otimes \mathrm{SO}(3) \otimes \mathbb{Z}_2 \otimes \mathbb{Z}_2 \sim \mathrm{SU}(2) \otimes \mathrm{SU}(2)$ symmetry, which is equivalent to O(4) symmetry [97]. Here the first SU(2) in the right-hand side refers to spin rotational symmetry, the second SU(2) pseudospin symmetry [98], the first $\mathbb{Z}_2$ in the left-hand side the usual particle-hole symmetry for both spin-up and spin-down electrons ($c_{i\sigma} \to (-1)^i c_{i\sigma}^{\dagger}$), and the second $\mathbb{Z}_2$ the particle-hole symmetry for spin-down electrons [$c_{i\downarrow} \to (-1)^i c_{i\downarrow}^{\dagger}$]. The pseudospin rotation can transform the CDW order $(1/N)\sum_i (-1)^i \langle c_{i\sigma}^{\dagger} c_{i\sigma}\rangle$ to the SC order $(1/N)\sum_i \langle c_{i\uparrow}^{\dagger} c_{i\downarrow}^{\dagger}\rangle$ [98], where $N = L \times L$ is the system size. The spin-down particle-hole symmetry can transform the usual AFM ordering into pseudospin-AFM ordering (pseudospin-AFM referring to CDW/SC) [99] so that AFM and pseudospin-AFM order parameters are degenerate. The Hubbard interaction $H_U = U\sum_i (n_{i\uparrow} - \frac{1}{2})(n_{i\downarrow} - \frac{1}{2})$, which breaks the second $\mathbb{Z}_2$ symmetry explicitly, can lift the degeneracy between the AFM and pseudospin-AFM ordering; AFM ordering is favored over pseudospin-AFM ordering by any finite (even infinitesimal) Hubbard repulsion $U > 0$.

The bond SSH model in Eq. (1) is sign-problem-free so that we can perform large-scale projector QMC simulations to investigate its ground-state phase diagram by varying phonon frequency ω and EPC constant λ. The projector QMC is numerically exact and is able to study the zero-temperature properties directly. Details of the projector QMC method can be found in the Supplemental Material [100]. We emphasize that the simulations here are free from the notorious sign problem [80] so that we can study large system size. To investigate various possible symmetry-breaking orders, we compute the structure factor $S(\boldsymbol{q}, L) = (1/N^2)\sum_{i,j} e^{i\boldsymbol{q}\cdot(\boldsymbol{r}_i - \boldsymbol{r}_j)}\langle \hat{O}_i \hat{O}_j\rangle$ of the corresponding order O and evaluate the RG-invariant ratio of the structure factor, namely, the correlation ratio, $R^S(L) = 1 - [S(\boldsymbol{Q} + \boldsymbol{\delta q}, L)/S(\boldsymbol{Q}, L)]$, where $\boldsymbol{Q}$ refers to the ordering momentum and $\boldsymbol{\delta q} = [(2\pi/L), (2\pi/L)]$ is a minimal momentum shift from $\boldsymbol{Q}$. For both Néel AFM and staggered VBS ordering, $\boldsymbol{Q} = (\pi, \pi)$. In the thermodynamic limit ($L \to \infty$), an ordered phase is recognized by $R^S \to 1$ while a disordered phase features $R^S \to 0$. For AFM ordering, we further compute the susceptibility ratio $R^{\chi}(L) = 1 - [\chi(\boldsymbol{Q} + \boldsymbol{\delta q}, L)/\chi(\boldsymbol{Q}, L)]$, where $\chi(\boldsymbol{q})$ represents magnetic susceptibility at momentum $\boldsymbol{q}$, as it has smaller finite-size corrections than the correlation ratio [101] (see the Supplemental Material [100] for technical details of evaluating susceptibilities).

Results in adiabatic and anti-adiabatic limit.—Integrating out phonons with finite frequency yields a retarded interaction between electrons. The retardation effect of EPC plays a central role in driving various novel physics, including SC. The retardation is usually characterized by the ratio between the phonon frequency ω and the Fermi energy or band width W. Before performing systematic QMC simulations on the SSH model at a generic finite phonon frequency, we first study the ground-state

properties at the adiabatic limit ($\omega = 0$) and anti-adiabatic limit ($\omega = \infty$), respectively.

In the adiabatic limit ($\omega = 0$), the phonon is static at zero temperature and the exact solution can be obtained by treating the phonon displacement configuration X_{ij} as variational parameters. As the electron's bare Fermi surface features a perfect nesting vector $\boldsymbol{Q} = (\pi, \pi)$, it is natural to expect that the Fermi surface is unstable towards staggered VBS ordering for any finite EPC constant λ. Indeed, our calculations show that the expectation value of electron hopping on NN bonds alternates in a staggered pattern (see the inset of Fig. 1), which breaks the lattice translational symmetry as well as $\mathbb{C}_4$ rotational symmetry (see the Supplemental Material [100] for details of the calculations).

In the anti-adiabatic (AA) limit ($\omega = \infty$), the effective electronic interaction mediated by phonons becomes instantaneous, which is proportional to the square of hopping on NN bonds. Consequently, in the AA limit, the original bond SSH model can be reduced to the following effective Hamiltonian by integrating out the phonons (see the Supplemental Material [100] for details of derivation):

$$H_{\mathrm{AA}} = -t\sum_{\langle ij\rangle}(c^{\dagger}_{i\sigma}c_{j\sigma} + \mathrm{H.c.}) + J\sum_{\langle ij\rangle}(\boldsymbol{S}_i\cdot\boldsymbol{S}_j + \tilde{\boldsymbol{S}}_i\cdot\tilde{\boldsymbol{S}}_j), \qquad (2)$$

where $J = 2g^2/K$ is the strength of instantaneous interactions mediated by optical phonons in the AA limit, $\boldsymbol{S}_i$ and $\tilde{\boldsymbol{S}}_i$ are spin and pseudospin operators on site i, respectively. Specifically, $\boldsymbol{S}_i = \frac{1}{2}c^{\dagger}_i\boldsymbol{\sigma}c_i$ and $\tilde{\boldsymbol{S}}_i = \frac{1}{2}\tilde{c}^{\dagger}_i\boldsymbol{\sigma}\tilde{c}_i$, where $c^{\dagger}_i = (c^{\dagger}_{i\uparrow}, c^{\dagger}_{i\downarrow})$, $\tilde{c}^{\dagger}_i = (c^{\dagger}_{i\uparrow}, (-1)^i c_{i\downarrow})$, and $\boldsymbol{\sigma}$ represents the vector of Pauli matrices. The phonon-mediated interactions include antiferromagnetic spin-exchange interaction, repulsive density-density interaction, and pair hopping terms. It is worth emphasizing that antiferromagnetic ($J > 0$) spin exchange interactions are generated by EPC of SSH phonons, yielding the possibility of AFM ordering at half filling. By performing QMC simulations on H_{AA}, we obtained the results of AFM correlation ratio and AFM order parameter as a function of EPC constant $\lambda = J/(2W)$, as shown in Fig. 2. The AFM correlation ratio R^S_{AFM} monotonically increases with the size L for all studied λ, as shown in Fig. 2(a), indicating that AFM ordering occurs for all $\lambda > 0$. Furthermore, we obtained the AFM order parameter by finite-size scaling to the thermodynamical limit, as shown in Fig. 2(b), which reveals that AFM order induced by SSH phonons increases with λ. Consequently, we conclude that the ground state of the bond SSH model in the AA limit possesses AFM long-range order for any $\lambda > 0$. Moreover, it is an AFM insulator as its Fermi surface is fully gapped by AFM order.

Antiferromagnetism at finite frequency.—We now study the quantum phase diagram of the SSH model of optical phonons with a generic finite frequency ($0 < \omega < \infty$).

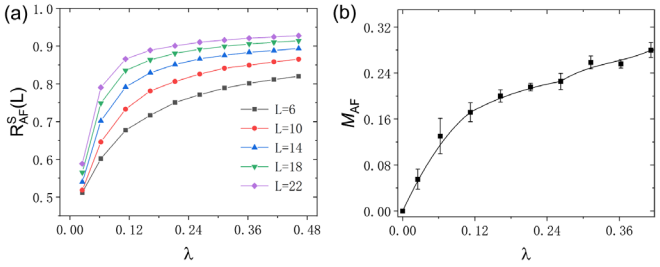

FIG. 2. The QMC results of AFM correlations in the anti-adiabatic limit ($\omega = \infty$). (a) The AFM correlation ratio R^S_{AFM} as a function of dimensionless EPC constant λ for different L. (b) The extrapolated AFM order parameter $M_{\mathrm{AFM}} = |\langle \boldsymbol{S}_i \rangle|$ to the thermodynamic limit ($L \to \infty$) as a function of λ. In the anti-adiabatic limit, AFM ordering occurs for any $\lambda > 0$. Note that CDW/SC correlation will be degenerate with AFM for $U = 0$, which is guaranteed by O(4) symmetry.

Since the ground-state is AFM in the AA limit ($\omega = \infty$) and VBS in the adiabatic limit ($\omega = 0$), there must be at least one quantum phase transition (QPT) between VBS and AFM phases when ω is varied from 0 to ∞. Indeed, for a given λ, our QMC simulations show that there is a direct QPT between AFM and VBS phases by varying ω. For $\lambda \approx 0.25$ ($g = 1.4$), the crossing of the VBS correlation ratio of different system sizes L implies that the VBS order persists from $\omega = 0$ to a critical frequency $\omega_c \approx 1.5$, as shown in Fig. 3(a). By evaluating dimer correlations on x or y bonds, as shown in Fig. 3(b), we further verified that the VBS ordering pattern for $0 < \omega < \omega_c$ is a staggered VBS breaking the lattice $\mathbb{C}_4$ symmetry, similar to the one observed in the adiabatic limit.

More interestingly, our QMC simulations show that the long-range AFM order emerges for $\omega > \omega_c$. Here the critical frequency ω_c can be accurately extracted from the crossing of AFM susceptibility ratio $R^{\chi}_{\mathrm{AFM}}(L)$ for different L. For $\lambda \approx 0.25$ ($g = 1.4$), the AFM susceptibility ratio $R^{\chi}_{\mathrm{AFM}}(L)$ displays good crossing near $\omega \approx 1.5$, as shown in Fig. 4(a), which implies that AFM order develops for $\omega > \omega_c$ with $\omega_c \approx 1.5$. To further verify the AFM phase

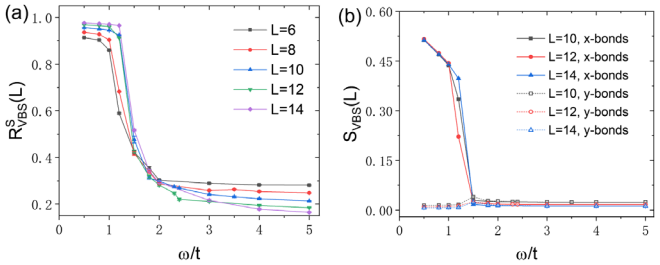

FIG. 3. The QMC results of VBS correlations as a function of ω for $\lambda \approx 0.25$ ($g = 1.4$). (a) The crossing of VBS correlation ratio R^S_{VBS} for different L implies that the VBS transition occurs at $\omega_c \approx 1.5$. (b) The VBS transition at $\omega_c \approx 1.5$ is also observed from the deviation between the structure factor of x-bond correlations and y-bond correlations.

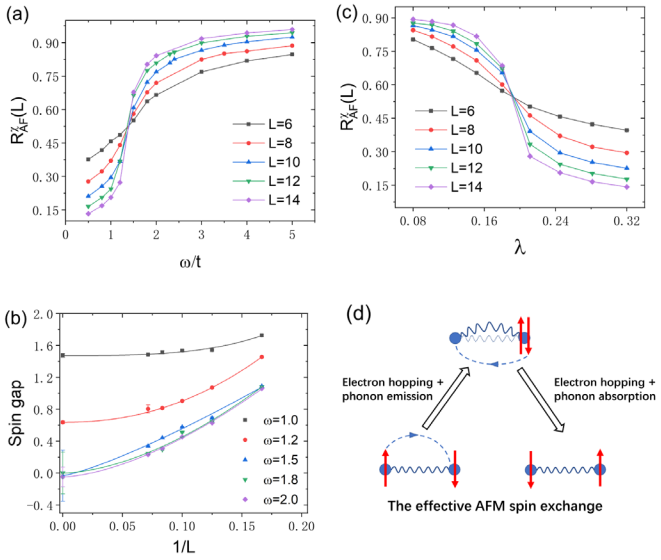

FIG. 4. (a) The QMC results of the AFM correlation ratio R^S_{AFM} as a function of ω for $\lambda \approx 0.25$ ($g = 1.4$). The crossing among curves with different L indicates that the AFM transition occurs at $\omega = \omega_c \approx 1.5$. The same result applies to pseudospin-AFM correlation for $U = 0$. (b) The finite size scaling of the spin gap for ω near the criticality ω_c. (c) For fixed $\omega = 1.0$, the AFM correlation ratio R^S_{AFM} as the function of λ and the AFM transition occurs at $\lambda_c \approx 0.18$. (d) The schematic picture of the second-order process of EPC which generates an effective retarded antiferromagnetic spin-exchange interactions.

with spontaneous spin-SU(2) rotational symmetry breaking, we compute the spin gap for ω around $\omega_c \approx 1.5$, as shown in Fig. 4(b). The spin gap is finite in the VBS regime, but it is extrapolated to zero in the AFM regime $\omega > \omega_c$, indicating the emergence of gapless spin-wave excitations as Goldstone modes of spin SU(2) symmetry breaking in the AFM phase. Taken together, these results convincingly show that the occurrence of phonon-induced AFM long-range order for $\omega > \omega_c$, where ω_c depends on λ.

Evidences of AFM ordering at $\omega > \omega_c(\lambda)$ are also obtained for various other EPC dimensionless parameters λ, from weak to strong, as plotted in Fig. 1. As the critical frequency $\omega_c(\lambda)$ increases monotonically with increasing λ, for a fixed frequency it is expected that the AFM phases should emerge in the regime of $\lambda < \lambda_c$ where λ_c is the critical EPC constant. Indeed, for the fixed frequency $\omega = 1.0$, AFM ordering is observed in the regime of $\lambda < \lambda_c \approx 0.18$ from the crossing of the AFM susceptibility ratio for different L, as shown in Fig. 4(c). The (π, π) AFM ordering fully gaps out the Fermi surface such that the ground state is an AFM insulator for $\lambda < \lambda_c$. As mentioned earlier, the bond SSH model at half-filling respects the O(4) symmetry, giving rise to the degeneracy between spin AFM and pseudospin AFM (namely, CDW/SC). The degeneracy can be lifted and spin AFM is more favored by turning on a weak repulsive Hubbard interaction, as shown in the QMC simulations of models with a weak Hubbard interaction (see the Supplemental Material [100] for details).

It is worth understanding heuristically why AFM ordering emerges for small λ. For sufficiently small λ, one can treat the electron-phonon coupling term g as a weak perturbation and the second-order process in g would generate a spin exchange process when the spin polarizations in the NN sites are opposite, as shown in Fig. 4(d). If the two spins on NN sites are parallel (namely, forming a triplet), the exchange process is not allowed. Since this second-order spin-exchange process can gain energy, the spin-exchange interaction is antiferromagnetic. A similar AFM exchange was also derived at strong coupling and anti-adiabatic limit in a 1D system [92]. This process provides a phonon mechanism to drive AFM ordering, which is qualitatively different from the usual AFM exchange mechanism of strong Hubbard Coulomb interaction. Note that phonon models such as the Holstein model with site phonons cannot directly generate AFM spin exchange.

To further corroborate our conclusion, we study how a weak Hubbard U affects spin AFM and pseudoospin-AFM ordering, as shown in Fig. 5. In Fig. 5(a) we obtain the magnetic moment in the thermodynamic limit for a range of weak U. It is clear that for $\lambda = 0.25$ the AFM ordering changes with U smoothly and the AFM moment is finite when U is reduced to zero. In contrast, for the pure Hubbard model without SSH phonons (namely, $\lambda = 0$), the AFM moment reduces to zero when U approaches zero. We fit the AFM moments obtained from our QMC simulations of the pure Hubbard model according to the asymptotic weak-coupling behavior $M \sim \mathrm{e}^{-A\sqrt{t/U}}$, where A is a constant. These results clearly indicate that EPC can induce a finite AFM ordering even when $U = 0$. In Fig. 5(b) we compare the spin and pseudospin AFM orders for $\lambda = 0.25$; the pseudospin-AFM order vanishes in the thermodynamic limit when a weak positive Hubbard U is turned on ($U/t \geq 0.05$ in our simulations). When $U = 0$, our simulations show that spin and pseudospin correlations

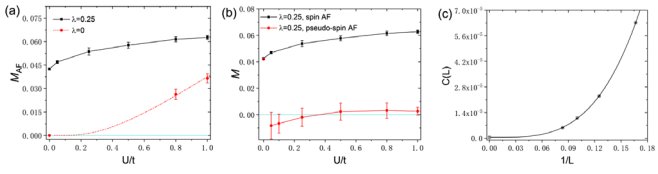

FIG. 5. QMC results of spin and pseudospin AFM order and their intercorrelation extrapolated to the thermodynamic limit. (a) The spin AFM order as a function of U for $\lambda = 0.25$ (fixing $\omega/t = 3.0$) and $\lambda = 0$. It clearly shows that the AFM order parameter is nonzero in the presence of SSH phonons even when $U = 0$. (b) The spin and pseudospin AFM orders as a function of U for $\lambda = 0.25$ and $\omega/t = 3.0$. (c) The finite size scaling of intercorrelation between AFM and pseudospin-AFM ordering at $\omega = 3t$ and $\lambda \approx 0.25$ ($g = 1.4t$) for $U = 0$.

are equal, as required by the O(4) symmetry of the underlining model. We emphasize that at $U = 0$ the degeneracy between the state with spin-AFM ordering and the state with pseudospin-AFM ordering does not necessarily mean that two orderings coexist. To check whether spin and pseudospin AFM orders coexist, we compute the intercorrelation between spin and pseudospin operators, as shown in Fig. 5(c) (see the Supplemental Material [100] for details). The intercorrelation obtained from QMC simulations is extrapolated to zero for $U = 0$ in the thermodynamic limit, which unambiguously indicates that spin-AFM and pseudospin-AFM orders do not coexist at $U = 0$, namely, the $\mathbb{Z}_2$ particle-hole symmetry of spin-down electrons is spontaneously broken in the ground state at $U = 0$.

Note that the model Eq. (1) at half-filling was also studied in Ref. [85]. The critical coupling strength for VBS ordering we obtained is consistent with the results in Ref. [85] for fixed phonon frequency. Nevertheless, Ref. [85] did not report the existence of AFM ordering. The absence of AFM ordering is possibly due to the fact that the QMC simulations in Ref. [85] were at finite temperature and spin-SU(2) rotational symmetry in two dimensions cannot be spontaneously broken at any finite temperature. In contrast, we performed zero-temperature QMC simulations which can directly access properties of the ground state of the 2D phonon model and observe a spontaneous spin-SU(2) symmetry breaking.

Conclusions and discussions.—We have systematically explored the ground-state phase diagram of the 2D bond SSH model taking account of full quantum phonon dynamics by zero-temperature QMC simulations. Remarkably, from the state-of-the-art numerically exact simulations, we have shown that the optical SSH phonons can induce a Néel AFM order when the phonon frequency is larger than a critical value ($\omega > \omega_c$) or the EPC constant is smaller than a critical value ($\lambda < \lambda_c$) [102]. The critical frequency ω_c can be much smaller than the band width W for weak or moderate EPC constant λ, which makes the phonon mechanism of AFM ordering practically feasible in realistic quantum materials. For instance, for the bond SSH model on the square lattice, we obtained $\omega_c/W \sim 0.1$ when $\lambda \approx 0.15$.

As mentioned above, the role of EPC in understanding the physics of strongly correlated materials, including cuprate and Fe-based high-temperature superconductors, has attracted increasing attention. We believe that our finding of optical SSH phonon induced AFM order may shed new light on understanding the cooperative effects of electronic correlations and EPC on the nature of AFM Mott physics. In a follow-up work [125], we shall present evidences that quantum SSH optical phonons can substantially enhance the d-wave pairing. We believe that these findings pave an important step to understanding the interplay of EPC and electronic correlations in strongly correlated materials including high-temperature superconductors.

We would like to thank Steve Kivelson, Dung-Hai Lee, and Yoni Schattner for helpful discussions. This work is supported in part by the NSFC under Grant No. 11825404 (X. C. and H. Y.), the MOSTC Grants No. 2018YFA0305604 and No. 2021YFA1400100 (H. Y.), Beijing Natural Science Foundation under Grant No. Z180010 (H. Y.), the CAS Strategic Priority Research Program under Grant No. XDB28000000 (H. Y.), Beijing Municipal Science and Technology Commission Grant No. Z181100004218001 (H. Y.), and the Gordon and Betty Moore Foundations EPiQS under Grant No. GBMF4545 (Z. X. L.).

*yaohong@tsinghua.edu.cn

[1] R. E. Peierls, *Quantum Theory of Solids* (Oxford University, New York/London, 1955).
[2] G. Grüner, Rev. Mod. Phys. **60**, 1129 (1988).
[3] W. P. Su, J. R. Schrieffer, and A. J. Heeger, Phys. Rev. Lett. **42**, 1698 (1979).
[4] A. J. Heeger, S. A. Kivelson, J. R. Schrieffer, and W. P. Su, Rev. Mod. Phys. **60**, 781 (1988).
[5] J. Bardeen, L. N. Cooper, and J. R. Schrieffer, Phys. Rev. **108**, 1175 (1957).
[6] J. R. Schrieffer, *Theory of Superconductivity* (W.A. Benjamin, San Francisco, 1964).
[7] I. Esterlis, B. Nosarzewski, E. W. Huang, B. Moritz, T. P. Devereaux, D. J. Scalapino, and S. A. Kivelson, Phys. Rev. B **97**, 140501(R) (2018).
[8] I. Esterlis, S. A. Kivelson, and D. J. Scalapino, Phys. Rev. B **99**, 174516 (2019).
[9] Z.-X. Li, M. L. Cohen, and D.-H. Lee, Phys. Rev. B **100**, 245105 (2019).
[10] N. C. Costa, T. Blommel, W.-T. Chiu, G. Batrouni, and R. T. Scalettar, Phys. Rev. Lett. **120**, 187003 (2018).
[11] Y.-X. Zhang, W.-T. Chiu, N. C. Costa, G. G. Batrouni, and R. T. Scalettar, Phys. Rev. Lett. **122**, 077602 (2019).
[12] C. Chen, X. Y. Xu, Z. Y. Meng, and M. Hohenadler, Phys. Rev. Lett. **122**, 077601 (2019).
[13] G. G. Batrouni and R. T. Scalettar, Phys. Rev. B **99**, 035114 (2019).
[14] B. Cohen-Stead, K. Barros, Z. Meng, C. Chen, R. T. Scalettar, and G. G. Batrouni, Phys. Rev. B **102**, 161108 (R) (2020).
[15] C. Feng and R. T. Scalettar, Phys. Rev. B **102**, 235152 (2020).
[16] Z. Li, G. Antonius, M. Wu, F. H. da Jornada, and S. G. Louie, Phys. Rev. Lett. **122**, 186402 (2019).
[17] M. Gao, X.-W. Yan, Z.-Y. Lu, and T. Xiang, Phys. Rev. B **101**, 094501 (2020).
[18] P. W. Anderson, Science **235**, 1196 (1987).
[19] S. A. Kivelson, I. P. Bindloss, E. Fradkin, V. Oganesyan, J. M. Tranquada, A. Kapitulnik, and C. Howald, Rev. Mod. Phys. **75**, 1201 (2003).
[20] P. W. Anderson, P. A. Lee, M. Randeria, T. M. Rice, N. Trivedi, and F. C. Zhang, J. Phys. Condens. Matter **16**, R755 (2004).
[21] P. A. Lee, N. Nagaosa, and X.-G. Wen, Rev. Mod. Phys. **78**, 17 (2006).
[22] D. J. Scalapino, Rev. Mod. Phys. **84**, 1383 (2012).

[23] J. C. S. Davis and D.-H. Lee, Proc. Natl. Acad. Sci. U.S.A. **110**, 17623 (2013).

[24] A. Lanzara, P. V. Bogdanov, X. J. Zhou, S. A. Kellar, D. L. Feng, E. D. Lu, T. Yoshida, H. Eisaki, A. Fujimori, K. Kishio, J.-I. Shimoyama, T. Noda, S. Uchida, Z. Hussain, and Z.-X. Shen, Nature (London) **412**, 510 (2001).

[25] Z.-X. Shen, A. Lanzara, S. Ishihara, and N. Nagaosa, Philos. Mag. B **82**, 1349 (2002).

[26] T. Cuk, F. Baumberger, D. H. Lu, N. Ingle, X. J. Zhou, H. Eisaki, N. Kaneko, Z. Hussain, T. P. Devereaux, N. Nagaosa, and Z.-X. Shen, Phys. Rev. Lett. **93**, 117003 (2004).

[27] A. S. Mishchenko and N. Nagaosa, Phys. Rev. Lett. **93**, 036402 (2004).

[28] X. J. Zhou *et al.*, Phys. Rev. Lett. **95**, 117001 (2005).

[29] T. Cuk, D. H. Lu, X. J. Zhou, Z.-X. Shen, T. P. Devereaux, and N. Nagaosa, Phys. Status Solidi B **242**, 11 (2005).

[30] O. Rösch, O. Gunnarsson, X. J. Zhou, T. Yoshida, T. Sasagawa, A. Fujimori, Z. Hussain, Z.-X. Shen, and S. Uchida, Phys. Rev. Lett. **95**, 227002 (2005).

[31] J. L. Tallon, R. S. Islam, J. Storey, G. V. M. Williams, and J. R. Cooper, Phys. Rev. Lett. **94**, 237002 (2005).

[32] J. Lee, K. Fujita, K. McElroy, J. A. Slezak, M. Wang, Y. Aiura, H. Bando, M. Ishikado, T. Masui, J.-X. Zhu, A. V. Balatsky, H. Eisaki, S. Uchida, and J. C. Davis, Nature (London) **442**, 546 (2006).

[33] S. Johnston, F. Vernay, B. Moritz, Z.-X. Shen, N. Nagaosa, J. Zaanen, and T. P. Devereaux, Phys. Rev. B **82**, 064513 (2010).

[34] S. Gerber *et al.*, Science **357**, 71 (2017).

[35] Y. He, M. Hashimoto, D. Song, S.-D. Chen, J. He, I. M. Vishik, B. Moritz, D.-H. Lee, N. Nagaosa, J. Zaanen, T. P. Devereaux, Y. Yoshida, H. Eisaki, D. H. Lu, and Z.-X. Shen, Science **362**, 62 (2018).

[36] B. Keimer, S. A. Kivelson, M. R. Norman, S. Uchida, and J. Zaanen, Nature (London) **518**, 179 (2015).

[37] Y.-H. Liu, R. M. Konik, T. M. Rice, and F.-C. Zhang, Nat. Commun. **7**, 10378 (2016).

[38] Y. Zhong, Y. Wang, S. Han, Y.-F. Lv, W.-L. Wang, D. Zhang, H. Ding, Y.-M. Zhang, L. Wang, K. He, R. Zhong, J. A. Schneeloch, G.-D. Gu, C.-L. Song, X.-C. Ma, and Q.-K. Xue, Sci. Bull. **61**, 1239 (2016).

[39] J.-Y. Chen, S. A. Kivelson, and X.-Q. Sun, Phys. Rev. Lett. **124**, 167601 (2020).

[40] C. Gadermaier, A. S. Alexandrov, V. V. Kabanov, P. Kusar, T. Mertelj, X. Yao, C. Manzoni, D. Brida, G. Cerullo, and D. Mihailovic, Phys. Rev. Lett. **105**, 257001 (2010).

[41] Y. He *et al.*, Phys. Rev. B **98**, 035102 (2018).

[42] Q.-Y. Wang, Z. Li, W.-H. Zhang, Z.-C. Zhang, J.-S. Zhang, W. Li, H. Ding, Y.-B. Ou, P. Deng, K. Chang, J. Wen, C.-L. Song, K. He, J.-F. Jia, S.-H. Ji, Y.-Y. Wang, L.-L. Wang, X. Chen, X.-C. Ma, and Q.-K. Xue, Chin. Phys. Lett. **29**, 037402 (2012).

[43] J. J. Lee, F. T. Schmitt, R. G. Moore, S. Johnston, Y.-T. Cui, W. Li, M. Yi, Z. K. Liu, M. Hashimoto, Y. Zhang, D. H. Lu, T. P. Devereaux, D.-H. Lee, and Z.-X. Shen, Nature (London) **515**, 245 (2014).

[44] Z.-X. Li, F. Wang, H. Yao, and D.-H. Lee, Sci. Bull. **61**, 925 (2016).

[45] Y. Wang, A. Linscheid, T. Berlijn, and S. Johnston, Phys. Rev. B **93**, 134513 (2016).

[46] Q. Song, T. L. Yu, X. Lou, B. P. Xie, H. C. Xu, C. H. P. Wen, Q. Yao, S. Y. Zhang, X. T. Zhu, J. D. Guo, R. Peng, and D. L. Feng, Nat. Commun. **10**, 758 (2019).

[47] S. Zhang, T. Wei, J. Guan, Q. Zhu, W. Qin, W. Wang, J. Zhang, E. W. Plummer, X. Zhu, Z. Zhang, and J. Guo, Phys. Rev. Lett. **122**, 066802 (2019).

[48] Y. Zhou and A. J. Millis, Phys. Rev. B **96**, 054516 (2017).

[49] W. Zhao, M. Li, C.-Z. Chang, J. Jiang, L. Wu, C. Liu, J. S. Moodera, Y. Zhu, and M. H. W. Chan, Sci. Adv. **4**, eaao2682 (2018).

[50] Z.-X. Li, T. P. Devereaux, and D.-H. Lee, Phys. Rev. B **100**, 241101(R) (2019).

[51] R. Peng, K. Zou, M. G. Han, S. D. Albright, H. Hong, C. Lau, H. C. Xu, Y. Zhu, F. J. Walker, and C. H. Ahn, Sci. Adv. **6**, eaay4517 (2020).

[52] D. Huang and J. E. Hoffman, Annu. Rev. Condens. Matter Phys. **8**, 311 (2017).

[53] D.-H. Lee, Annu. Rev. Condens. Matter Phys. **9**, 261 (2018).

[54] Z. Han, S. A. Kivelson, and H. Yao, Phys. Rev. Lett. **125**, 167001 (2020).

[55] F. F. Assaad, M. Imada, and D. J. Scalapino, Phys. Rev. Lett. **77**, 4592 (1996).

[56] F. F. Assaad, M. Imada, and D. J. Scalapino, Phys. Rev. B **56**, 15001 (1997).

[57] A. Macridin, G. A. Sawatzky, and M. Jarrell, Phys. Rev. B **69**, 245111 (2004).

[58] P. Werner and A. J. Millis, Phys. Rev. Lett. **99**, 146404 (2007).

[59] S. Johnston, E. A. Nowadnick, Y. F. Kung, B. Moritz, R. T. Scalettar, and T. P. Devereaux, Phys. Rev. B **87**, 235133 (2013).

[60] T. Ohgoe and M. Imada, Phys. Rev. Lett. **119**, 197001 (2017).

[61] N. C. Costa, K. Seki, S. Yunoki, and S. Sorella, arXiv: 1910.01146.

[62] P. Sengupta, A. W. Sandvik, and D. K. Campbell, Phys. Rev. B **67**, 245103 (2003).

[63] N. C. Costa, K. Seki, and S. Sorella, Phys. Rev. Lett. **126**, 107205 (2021).

[64] M. Hohenadler and G. G. Batrouni, Phys. Rev. B **100**, 165114 (2019).

[65] C. Wang, Y. Schattner, and S. A. Kivelson, Phys. Rev. B **104**, 081110 (2021).

[66] C. Honerkamp, H. C. Fu, and D.-H. Lee, Phys. Rev. B **75**, 014503 (2007).

[67] J. P. Hague, P. E. Kornilovitch, J. H. Samson, and A. S. Alexandrov, Phys. Rev. Lett. **98**, 037002 (2007).

[68] D. Wang, W.-S. Wang, and Q.-H. Wang, Phys. Rev. B **92**, 195102 (2015).

[69] Y. Wang, I. Esterlis, T. Shi, J. I. Cirac, and E. Demler, Phys. Rev. Research **2**, 043258 (2020).

[70] J. Lee, S. Zhang, and D. R. Reichman, Phys. Rev. B **103**, 115123 (2021).

[71] R. Blankenbecler, D. J. Scalapino, and R. L. Sugar, Phys. Rev. D **24**, 2278 (1981).

[72] F. Assaad and H. Evertz, World-line and determinantal quantum monte carlo methods for spins, phonons and electrons, in *Computational Many-Particle Physics*, edited by H. Fehske, R. Schneider, and A. Weiße (Springer Berlin Heidelberg, Berlin, Heidelberg, 2008), pp. 277–356.

[73] Z.-X. Li, Y.-F. Jiang, and H. Yao, Phys. Rev. B **91**, 241117(R) (2015).
[74] Z.-X. Li, Y.-F. Jiang, and H. Yao, Phys. Rev. Lett. **117**, 267002 (2016).
[75] Z. C. Wei, C. Wu, Y. Li, S. Zhang, and T. Xiang, Phys. Rev. Lett. **116**, 250601 (2016).
[76] E. Berg, M. A. Metlitski, and S. Sachdev, Science **338**, 1606 (2012).
[77] C. Wu and S.-C. Zhang, Phys. Rev. B **71**, 155115 (2005).
[78] M. Troyer and U.-J. Wiese, Phys. Rev. Lett. **94**, 170201 (2005).
[79] L. Wang, Y.-H. Liu, M. Iazzi, M. Troyer, and G. Harcos, Phys. Rev. Lett. **115**, 250601 (2015).
[80] Z.-X. Li and H. Yao, Annu. Rev. Condens. Matter Phys. **10**, 337 (2019).
[81] J. K. Freericks and E. H. Lieb, Phys. Rev. B **51**, 2812 (1995).
[82] Y. Ono and T. Hamano, J. Phys. Soc. Jpn. **69**, 1769 (2000).
[83] S. Beyl, F. Goth, and F. F. Assaad, Phys. Rev. B **97**, 085144 (2018).
[84] S. Li and S. Johnston, npj Quantum Mater. **5**, 40 (2020).
[85] B. Xing, W.-T. Chiu, D. Poletti, R. T. Scalettar, and G. Batrouni, Phys. Rev. Lett. **126**, 017601 (2021).
[86] E. Fradkin and J. E. Hirsch, Phys. Rev. B **27**, 1680 (1983).
[87] P. Sengupta, A. W. Sandvik, and D. K. Campbell, Phys. Rev. B **67**, 245103 (2003).
[88] H. Bakrim and C. Bourbonnais, Phys. Rev. B **76**, 195115 (2007).
[89] D. J. J. Marchand, G. De Filippis, V. Cataudella, M. Berciu, N. Nagaosa, N. V. Prokof'ev, A. S. Mishchenko, and P. C. E. Stamp, Phys. Rev. Lett. **105**, 266605 (2010).
[90] M. Hohenadler, F. F. Assaad, and H. Fehske, Phys. Rev. Lett. **109**, 116407 (2012).
[91] A. Nocera, J. Sous, A. E Feiguin, and M. Berciu, arXiv: 2008.03304.
[92] J. Sous, M. Chakraborty, R. V. Krems, and M. Berciu, Phys. Rev. Lett. **121**, 247001 (2018).
[93] M. Weber, F. F. Assaad, and M. Hohenadler, Phys. Rev. B **91**, 245147 (2015).
[94] M. Weber, Phys. Rev. B **103**, L041105 (2021).
[95] M. Weber, F. Parisen Toldin, and M. Hohenadler, Phys. Rev. Research **2**, 023013 (2020).
[96] S. Barisic, J. Labbé, and J. Friedel, Phys. Rev. Lett. **25**, 919 (1970).
[97] C. N. Yang and S.-C. Zhang, Mod. Phys. Lett. B **4**, 759 (1990).
[98] S.-C. Zhang, Phys. Rev. Lett. **65**, 120 (1990).
[99] E. Fradkin, *Field Theories of Condensed Matter Physics*, 2nd ed. (Cambridge University Press, Cambridge, England, 2013).
[100] See Supplemental Material at http://link.aps.org/supplemental/10.1103/PhysRevLett.127.247203 for details, including Monte Carlo simulations, the derivation of the effective Hamiltonian, mean-field calculations, finite-size analysis, the effect of repulsive Hubbard interaction, and the definition of intercorrelations.
[101] F. Parisen Toldin, M. Hohenadler, F. F. Assaad, and I. F. Herbut, Phys. Rev. B **91**, 165108 (2015).
[102] We have shown evidences of a direct QPT between the AFM and VBS phases. It is natural to ask if the direct QPT between AFM and VBS phases here is first order or continuous. Since AFM and VBS phases break totally different symmetries, the QPT between them is putatively first order in the Landau paradigm although it would be intriguing to explore if a deconfined quantum critical point (DQCP) [103,104] occurs in this case. The phenomena of DQCP have been extensively studied for QPTs between Néel AFM and columnar VBS [105–115]. More recently, it has been argued from duality relations that, at such a transition point, the SO(5) symmetry might emerge at low energy [116–121]. However, the VBS order in the bond SSH model studied here is the staggered one, for which the VBS Z_4 vortex is featureless, namely, not carrying a spinon [122,123]. Consequently, a (possibly weak) first-order transition instead of DQCP [124] would be expected for the QPT between AFM and staggered VBS phases in the phonon model under study.
[103] T. Senthil, A. Vishwanath, L. Balents, S. Sachdev, and M. P. A. Fisher, Science **303**, 1490 (2004).
[104] T. Senthil, L. Balents, S. Sachdev, A. Vishwanath, and M. P. A. Fisher, Phys. Rev. B **70**, 144407 (2004).
[105] A. W. Sandvik, Phys. Rev. Lett. **98**, 227202 (2007).
[106] R. G. Melko and R. K. Kaul, Phys. Rev. Lett. **100**, 017203 (2008).
[107] S. Pujari, K. Damle, and F. Alet, Phys. Rev. Lett. **111**, 087203 (2013).
[108] H. Shao, W. Guo, and A. W. Sandvik, Science **352**, 213 (2016).
[109] R. K. Kaul, R. G. Melko, and A. W. Sandvik, Annu. Rev. Condens. Matter Phys. **4**, 179 (2013).
[110] L. Wang, Z.-C. Gu, F. Verstraete, and X.-G. Wen, Phys. Rev. B **94**, 075143 (2016).
[111] N. Ma, Y.-Z. You, and Z. Y. Meng, Phys. Rev. Lett. **122**, 175701 (2019).
[112] Y. Liu, Z. Wang, T. Sato, M. Hohenadler, C. Wang, W. Guo, and F. F. Assaad, Nat. Commun. **10**, 2658 (2019).
[113] Z.-X. Li, S.-K. Jian, and H. Yao, arXiv:1904.10975.
[114] R. Ma and C. Wang, Phys. Rev. B **102**, 020407(R) (2020).
[115] A. Nahum, Phys. Rev. B **102**, 201116(R) (2020).
[116] A. Nahum, P. Serna, J. T. Chalker, M. Ortuño, and A. M. Somoza, Phys. Rev. Lett. **115**, 267203 (2015).
[117] C. Wang and T. Senthil, Phys. Rev. X **5**, 041031 (2015).
[118] C. Wang, A. Nahum, M. A. Metlitski, C. Xu, and T. Senthil, Phys. Rev. X **7**, 031051 (2017).
[119] M. A. Metlitski and A. Vishwanath, Phys. Rev. B **93**, 245151 (2016).
[120] N. Seiberg, T. Senthil, C. Wang, and E. Witten, Ann. Phys. (Amsterdam) **374**, 395 (2016).
[121] Y. Q. Qin, Y.-Y. He, Y.-Z. You, Z.-Y. Lu, A. Sen, A. W. Sandvik, C. Xu, and Z. Y. Meng, Phys. Rev. X **7**, 031052 (2017).
[122] M. Levin and T. Senthil, Phys. Rev. B **70**, 220403(R) (2004).
[123] C. Xu and L. Balents, Phys. Rev. B **84**, 014402 (2011).
[124] A. Sen and A. W. Sandvik, Phys. Rev. B **82**, 174428 (2010).
[125] X. Cai, Z.-X. Li, and H. Yao (to be published).